

# Ratchet transport of interacting particles

A.D.Chepelianskii,<sup>1</sup> M.V.Entin,<sup>2</sup> L.I.Magarill,<sup>2</sup> and D.L.Shepelyansky<sup>3</sup>

<sup>1</sup>*Laboratoire de Physique des Solides, UMR CNRS 8502, Bât. 510, Université Paris-Sud, 91405 Orsay, France*

<sup>2</sup>*Institute of Semiconductor Physics, Siberian Division of Russian Academy of Sciences, Novosibirsk, 630090, Russia*

<sup>3</sup>*Laboratoire de Physique Théorique - IRSAMC, UPS & CNRS, Université de Toulouse, 31062 Toulouse, France*

(Dated: August 21, 2008; Revised: September 17, 2008)

We study analytically and numerically the ratchet transport of interacting particles induced by a monochromatic driving in asymmetric two-dimensional structures. The ratchet flow is preserved in the limit of strong interactions and can become even stronger compared to the non-interacting case. The developed kinetic theory gives a good description of these two limiting regimes. The numerical data show emergence of turbulence in the ratchet flow under certain conditions.

PACS numbers: 05.60.-k, 47.61.-k, 72.40.+w

## I INTRODUCTION

For systems without spatial inversion symmetry the appearance of directed flow of particles induced by a time-periodic parameter variation with a zero-mean force is now commonly known as the ratchet effect (see reviews [1, 2, 3]). This phenomenon is ubiquitous in nature so that such flows appear in a variety of systems including asymmetric crystals [4, 5] and semiconductor surfaces [6] under light radiation, vortices in Josephson junction arrays [7], macroporous silicon membranes [8], microfluidic channels [9] and others. A significant increase of interest to ratchets is related to the experimental progress in the investigation of molecular transport in biological systems like proteins characterized by asymmetry and non-equilibrium [1, 2, 3]. At the same time the nanotechnology development allowed to fabricate artificial asymmetric nanostructures with the two-dimensional electron gas (2DEG) where it has been shown that infrared or microwave radiation creates a ratchet transport [10, 11, 12, 13]. The theoretical studies predicted that the directionality of ratchet flow in such systems can be controlled by the polarization of radiation [14, 15, 16, 17, 18] that has been confirmed by recent experiments with a semi-disk Galton board for 2DEG in AlGaAs/GaAs heterojunctions [19].

Till present the theoretical studies of ratchet transport have been done mainly for non-interacting particles [1, 2, 3, 4, 5, 14, 18]. However, in many systems the interactions between particles are of primary importance like for example for microfluidic channels [9], 2DEG nanostructures with strong electron-electron ( $e$ - $e$ ) interactions at a large  $r_s$  parameter [20], granulated materials [21] and one-dimensional Luttinger liquids [22]. On a first glance it seems that a strong scattering between particles should suppress the ratchet transport. But on the other hand the local conservation of momentum of particles indicates that even in presence of strong interactions the ratchet flow still should exist. The investigation of the properties of ratchet transport for interacting particles in two dimensions is the main aim of this paper. The theory

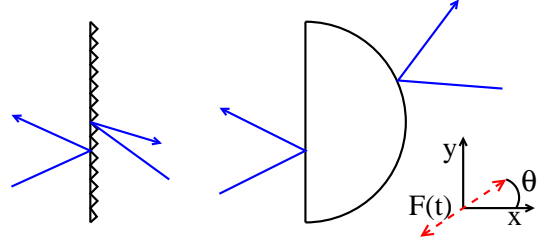


FIG. 1: (color online) Geometry of asymmetric scatterers oriented in  $(x, y)$ -plane: cuts with elastic (left) and diffusive (right) sides; elastic semidisks; liner-polarized force  $\mathbf{F}$  has angle  $\theta$  in respect to  $x$ -axis.

developed is based on the kinetic approach used in [18] extended to the case of strong interactions. The theory is compared with the extensive numerical simulations of ratchet transport of interacting particles in asymmetric structures. The model description is given in Section II; the analytical theory based on the kinetic equation is developed in Section III; the numerical results are presented in Section IV and the discussion is given in Section V.

## II MODEL DESCRIPTION

The interactions between particles are treated in the frame of the mesoscopic multi-particle collision model (MMPCM) proposed by Kapral (see e.g. [23]). This method exactly preserves the total momentum and energy of particles colliding inside each of  $N_{cel}$  collision cells on which the whole coordinate space with  $N$  particles is divided. In this method the collisions inside cells are modeled by rotation of all particle velocities in the moving center of mass frame of a given cell on a random angle after a time  $\tau_K$ . To equilibrate the whole system of interacting particles in presence of external monochromatic driving force  $\mathbf{F} \cos \omega t$  we use the Nosè-Hoover thermostat [24] which drives the system to the Boltzmann equilibrium with a temperature  $T = mv_T^2/2$  on a relaxation time  $\tau_H$ . Such a combination of two methods for systems with interactions and  $ac$ -driving has been already

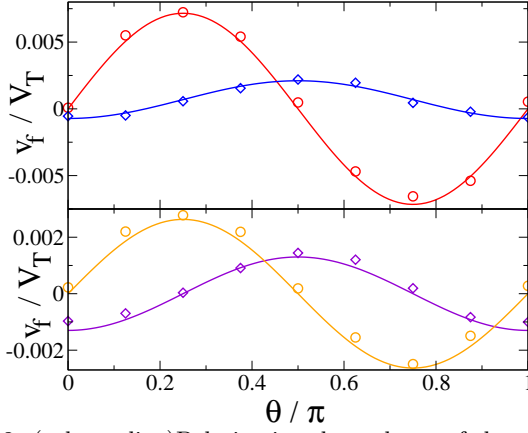


FIG. 2: (color online) Polarization dependence of the average ratchet flow  $\mathbf{v}_f$  in the flashing cuts model with (top panel) and without (bottom panel) interactions; diamonds and circles show numerical data for  $v_{f,x}$  and  $v_{f,y}$  components, curves give the fits of data (see text). The system parameters are:  $N = 10^4$ ,  $N_{cel} = 100 \times 100$  inside the periodic space domain  $R \times R$  with  $v_T \tau_H / R = 2.4$ ,  $\tau_c / \tau_H = 0.45$ ,  $\tau_K / \tau_H = 0.02$ ,  $\omega \tau_H = 3$ ,  $F v_T \tau_c / T = 0.64$  for the top panel and same parameters for the bottom panel but  $\tau_K / \tau_H = \infty$  and impurity scattering is added with  $\tau_{im} / \tau_H = 0.5$ ; total integration time is  $t / \tau_H \approx 10^3$ .

used in [25]. As in [18] the asymmetry appears due to asymmetric scatterers having form of vertical cuts with diffusive (right) and elastic (left) sides (cuts model) or of elastic semi-disks of radius  $r_d$  (semi-disks model) placed in a periodic square lattice of size  $R \times R$ . The system orientation geometry and two types of scatterers are shown in Fig.1 (see also [18] and Fig. 5 below). In the cuts model it is assumed that the scattering on cuts takes place instantaneously at random moments of time which have a Poisson distribution with time scale  $\tau_c$ . This corresponds to the case of flashing cuts model (instantaneous appearance of cut at some moment of time) which is slightly different from the case of static cuts randomly distributed in the plane (both cases were discussed in [18]). As in [18], in absence of interactions an effective impurity scattering is added with the scattering time  $\tau_{im}$ . The monochromatic force is polarized as it is shown in Fig. 1 with  $\mathbf{F} = F(\cos \theta, \sin \theta)$ . Here, we present numerical results only for the semidisks model and the flashing cuts model, which is rather convenient for numerical simulations, but in the analytical treatment we also consider the static cuts model.

The results of numerical simulations for the polarization dependence of the ratchet flow in the flashing cuts model are shown in Fig. 2. In absence of interactions the results are well described by the theory [18] with the fit dependence  $\mathbf{v}_f / v_T = b(-\cos(2\theta), 2\sin(2\theta))/2$  where  $b = 0.0064(F v_T \tau_c / T)^2 \approx 0.8b_{th}$  and  $b_{th}$  is the theory value (see Eqs.(9),(41) in [18]). For interacting particles the fit gives the dependence  $\mathbf{v}_f / v_T = b_{int}(-a_1 \cos^2 \theta + a_2 \sin^2 \theta, \sin(2\theta))$  with  $b_{int}/b = 2.7$  and  $a_1 = 0.10, a_2 =$

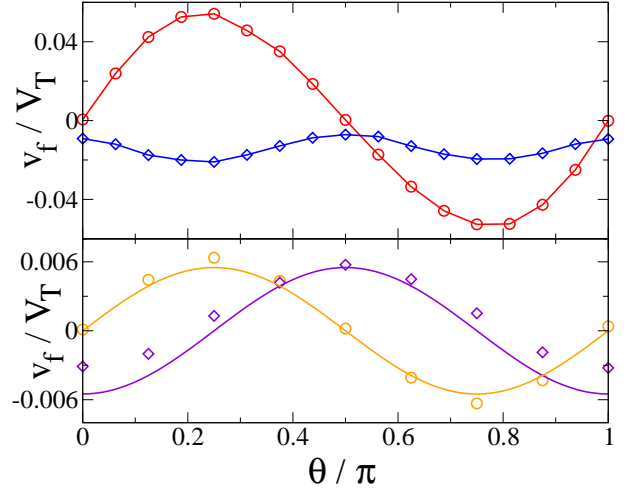


FIG. 3: (color online) Same as in Fig. 2 for the semi-disk model with  $R/r_d = 4$ ,  $F r_d / T = 0.15$ ,  $\omega \tau_H = 1$ , effective  $\tau_c / \tau_H \approx R^2 / (2r_d v_T \tau_H) = 0.85$ , other parameters are as in Fig. 2.

0.29. In presence of interactions the ratchet flow appears even after polarization averaging. The results for the semi-disks model are shown in Fig. 3. Without interactions the data are satisfactory described by the theoretical dependence  $\mathbf{v}_f / v_T = b(-\cos(2\theta), \sin(2\theta))$  with the fitting value  $b = 0.24(F r_d / T)^2 \approx 0.4b_{th}$  and the theoretical value  $b_{th}$  of [18] (see Eq.(42) and discussion there). In presence of interactions the polarization dependence of the flow is qualitatively changed: the component  $v_y$  is enhanced by a factor 8 and  $v_x$  remains negative for all  $\theta$  showing signature of 4th  $\theta$ -harmonic (Fig. 3, top panel, curves are drawn to adapt an eye).

### III ANALYTICAL THEORY

The numerical simulations are based on the dynamical description of motions of many interacting particles. To obtain an analytical description of the ratchet transport we use the kinetic equation approach valid for systems with developed chaos and rapid decay of correlations. The validity of the kinetic equation requires rare collisions with asymmetric scatterers (antidots) and randomness of scattering events. Under such conditions the kinetic equation can be applied for comparative study with the numerical data even if the numerical simulations are done for a deterministic system with a periodic lattice of semi-disks of relatively large size.

The symmetry of the system determines the ratchet flow which mean velocity  $\mathbf{v}_f$  is quadratic in the amplitude of the *ac*-force  $\mathbf{F}(t) = \text{Re}(\mathbf{F}e^{-i\omega t})$ . Therefore, the flow velocity can be described by the phenomenological expressions

$$v_{f,x} = \alpha_{xxx}|F_x|^2 + \alpha_{xyy}|F_y|^2, \quad v_{f,y} = 2\text{Re}(\alpha_{xyy}F_x F_y^*).$$

The tensor components  $\alpha_{xxx}$ ,  $\alpha_{xyy}$  and  $\text{Re}(\alpha_{yxy})$  determine the response produced by a linear-polarized monochromatic force ( $\text{Im}\mathbf{F} = 0$ ). In absence of interactions (see [18]), for the linear polarization along  $x$  or  $y$  axes the mean flow is directed along  $x$ -axis; the current in  $y$  direction appears for tilted linear-polarized force.

We also note that for the elliptically-polarized force with  $\text{Im}\mathbf{F} \neq 0$  there exists also a circular ratchet effect determined by the product of  $\text{Im}(\alpha_{yxy})$  and  $\text{Im}(F_x F_y^*)$  but we will not consider this effect here.

### Kinetic equation

The kinetic equation in the momentum space  $\mathbf{p}$  reads

$$\frac{\partial f}{\partial t} + \mathbf{F}(t) \frac{\partial f}{\partial \mathbf{p}} = \hat{I}(f). \quad (1)$$

where in the case of microwave field,  $\mathbf{E}(t)$  is the electric field  $\mathbf{E}(t)$  interacting with electron gas  $\mathbf{F}(t) = e\mathbf{E}(t)$ ,  $e$  is the electron charge. The collision operator  $\hat{I} = \hat{I}_{el} + \hat{I}_{ee}$  contains the operator of elastic collisions (including impurities and scatterers (or antidots))  $\hat{I}_{el}$  and interparticle (electron-electron or  $e$ - $e$ ) collisions  $\hat{I}_{ee}$ .

The integral of elastic collisions with scatterers and static impurities reads as

$$\hat{I}_{el}(f_{\mathbf{p}}) = \sum_{\mathbf{p}'} Q_{\mathbf{p}\mathbf{p}'} f_{\mathbf{p}'} = \sum_{\mathbf{p}'} [W(\mathbf{p}', \mathbf{p}) f_{\mathbf{p}'} - W(\mathbf{p}, \mathbf{p}') f_{\mathbf{p}}], \quad (2)$$

where  $Q_{\mathbf{p}\mathbf{p}'}$  is the kernel of the operator  $\hat{I}_{el}$  and  $W(\mathbf{p}', \mathbf{p})$  is the probability of the transition from  $\mathbf{p}'$  to  $\mathbf{p}$ .

The interparticle collisions operator ( $e$ - $e$ ) operator is

$$\begin{aligned} \hat{I}_{ee}(f) = & \frac{2\pi}{S^2} \sum_{\mathbf{p}_1, \mathbf{p}', \mathbf{p}_1'} \delta_{\mathbf{p}+\mathbf{p}_1, \mathbf{p}'+\mathbf{p}_1'} \\ & \times \delta(\epsilon_{\mathbf{p}} + \epsilon_{\mathbf{p}_1} - \epsilon_{\mathbf{p}'} - \epsilon_{\mathbf{p}_1'}) u_{\mathbf{p}-\mathbf{p}'}^2 \\ & \times \{f_{\mathbf{p}'} f_{\mathbf{p}_1'} (1 - f_{\mathbf{p}})(1 - f_{\mathbf{p}_1}) - f_{\mathbf{p}} f_{\mathbf{p}_1} (1 - f_{\mathbf{p}'})(1 - f_{\mathbf{p}_1'})\}. \end{aligned} \quad (3)$$

Here  $S$  is the sample area,  $u_{\mathbf{k}}$  is the Fourier transform of  $e$ - $e$ -interactions.

Interparticle collisions satisfy the conservation of the total momentum of gas. Due to the Galileo invariance the action of the collision integral on the equilibrium distribution function with shifted argument  $\hat{I}_{ee} f_{\mathbf{p}+\mathbf{a}}^{(0)}$  vanishes for any  $\mathbf{a}$ . Expanding by  $\mathbf{a}$  we have:

$$\begin{aligned} \hat{I}_{ee}(f_{\mathbf{p}}^{(0)}) &= 0, \quad \hat{I}_{ee}'(\mathbf{a} \partial_{\mathbf{p}} f^{(0)}) = 0, \\ \hat{I}_{ee}''(\mathbf{a} \partial_{\mathbf{p}} f^{(0)} * \mathbf{a} \partial_{\mathbf{p}'} f^{(0)}) &+ \hat{I}_{ee}'(a_i a_j \partial_{p_i, p_j}^2 f^{(0)}) = 0. \end{aligned} \quad (4)$$

We use the following notations for the first and the second variations around equilibrium:  $\delta \hat{I}_{ee}(f) = \hat{I}_{ee}'(\delta f)$  (linear operator),  $\delta^2 \hat{I}_{ee}(f) = \hat{I}_{ee}''(\delta f * \delta f)$  (bi-linear operator, asterisk denotes integration with two functions of different arguments).

The ratchet flow is generated by the anisotropy of collisions. This anisotropy is constructed artificially due to asymmetric form of oriented scatterers. As theoretical models we considered cases of fixed oriented anisotropic scatterers, namely cuts and semidisks. The model of static cuts is analytically solvable [18] but has a disadvantage since it leads to a divergence due to electrons moving along the mirrors. Even if this divergence can be regularized by an isotropic impurity scattering such a property is not very convenient. Due to that it is useful to use a modified model of flashing cuts which does not have such divergence. In this model at any moment a particle can meet a scatterer with a constant probability independent of its velocity and direction of motion; after collision the particle equi-probably scatters into any angle of the right semicircle if it collides from the right semicircle and is mirror-reflected if it collides from left semicircle (see Fig.1). Such a model of flashing cuts gives a significant simplification for analytical and numerical studies.

The corresponding transition probability in these models are given by (see also [18]):

$$W(\mathbf{p}', \mathbf{p}) = \frac{4\pi^2}{mS} w(\varphi', \varphi) \delta(\epsilon_{\mathbf{p}} - \epsilon_{\mathbf{p}'}); \quad (5)$$

with

$$\begin{aligned} w(\varphi', \varphi) = & \frac{1}{\tau_c} \left[ \cos \varphi' \theta(\cos \varphi') \delta(\varphi' + \varphi - \pi) \right. \\ & \left. - \frac{1}{2} \cos \varphi' \cos \varphi \theta(\cos \varphi) \theta(-\cos \varphi') \right] \quad (\text{static cuts}), \end{aligned} \quad (6)$$

$$\begin{aligned} w(\varphi', \varphi) = & \frac{1}{\tau_c} \left[ \cos \varphi' \theta(\cos \varphi') \delta(\varphi' + \varphi - \pi) + \right. \\ & \left. \frac{1}{4} \left| \sin \left( \frac{\varphi - \varphi'}{2} \right) \right| [\theta(\varphi - \varphi') \theta(-\varphi - \varphi') \right. \\ & \left. + \theta(\varphi' - \varphi) \theta(\varphi + \varphi')] \right] \quad (\text{semi-disks}), \end{aligned} \quad (7)$$

$$\begin{aligned} w(\varphi', \varphi) = & \frac{1}{\tau_c} [\theta(\cos \varphi') \delta(\varphi' + \varphi - \pi) + \\ & \frac{1}{\pi} \theta(\cos \varphi) \theta(-\cos \varphi')] \quad (\text{flashing cuts}). \end{aligned} \quad (8)$$

Here  $\varphi$  is the polar angle of electron momentum ( $-\pi < \varphi < \pi$ ),  $\tau_c(\varepsilon)$  is the characteristic scattering time on asymmetric scatterers,  $\theta(x)$  is the Heaviside function.

### Linear response

We consider the limit of high rate of interparticle scattering exceeding the rate of elastic collisions. At the same time the interactions preserve the total momentum and in isotropic media do not affect the momentum relaxation. This is not the case for an anisotropic medium

where the interactions indirectly lead to the momentum relaxation due to the conversion of the first angular harmonic of the distribution function  $f_{\mathbf{p}}$  to higher harmonics produced by the anisotropic scattering. In particular, it is generally expected that in an isotropic medium with closed Fermi surface the e-e scattering does not affect the conductivity. Nevertheless, in the considered case of anisotropic medium e-e collisions indirectly affect the momentum relaxation rate. This action is realized due to the conversion of the first angular harmonics of the distribution function to higher harmonics produced by the anisotropic scattering. As a result, the conductivity becomes temperature dependent in the temperature range when the e-e relaxation time is comparable with the elastic relaxation time.

At first we consider the linear response to the electric field using the expansion  $f = f^{(0)} + f^{(1)} + f^{(2)} + \dots$  in small driving force  $F$ . The linearized kinetic equation can be written in the form  $(f^{(1)}(t) = \text{Re}(f_{\omega}^{(1)} e^{i\omega t}))$ :

$$-i\omega f_{\omega}^{(1)} + \mathbf{F}_{\omega} \partial_{\mathbf{p}} f^{(0)} = \hat{I}^{(1)}(f_{\omega}^{(1)}), \quad (9)$$

where the collision operator contains the elastic collisions with anisotropic scatterers determined by  $\hat{I}_{el}$  and inter-particle or  $e$ - $e$  collisions determined by  $\hat{I}'_{ee}$ :

$$\hat{I}^{(1)} = \hat{I}_{el} + \hat{I}'_{ee} \quad (10)$$

The formal solution of Eq.(9) in the first order of alternating force is

$$f_{\omega}^{(1)} = (i\omega + \hat{I}^{(1)})^{-1} (\mathbf{F}_{\omega} \partial_{\mathbf{p}}) f^{(0)}. \quad (11)$$

In the case of weak e-e interaction  $\hat{I}'_{ee}$  can be canceled. In the opposite limit of strong e-e scattering the formal parameter describing  $\hat{I}_{ee}$  is large. Having in mind Eq. (4) we see that the inverse operator  $(\omega + \hat{I}^{(1)})^{-1}$  can be found by a projection on the subspace of the Hilbert space of the basis functions  $\psi_i = \frac{\partial f^{(0)}}{\partial p_i} / \|\frac{\partial f^{(0)}}{\partial p_i}\|$  corresponding to zero eigenvalue of the operator  $\hat{I}'_{ee}$ . Thus the operator  $\hat{I}_{el}$  is replaced by its projection, while  $\hat{I}'_{ee}$  can be canceled. The resulting tensor of conductivity of  $e$ -charged particles with density  $n_e$  reads

$$\sigma_{ij}(\omega) = \frac{e^2 n_e}{m} \frac{\tau_i}{1 - i\omega\tau_i} \delta_{ij}, \quad (12)$$

where  $\tau_i$  are relaxation times of the first harmonics of the distribution function related with the projected operator of elastic collisions:

$$\frac{1}{\tau_i} = - \sum_{\mathbf{p}, \mathbf{p}'} \psi_i(\mathbf{p}) Q_{\mathbf{p}\mathbf{p}'} \psi_i(\mathbf{p}'). \quad (13)$$

Here in  $\tau_i$  index  $i$  is axis index ( $x$  or  $y$ ). For the considered systems from the relations (6)-(8) we have  $\tau_i = \bar{\tau}_c/a_i$

and

$$\begin{aligned} a_x &= \frac{\pi}{8} + \frac{4}{\pi}, & a_y &= \frac{2}{3\pi} & (\text{for static cuts}), \\ a_x &= \frac{2}{3} + \frac{8}{3\pi}, & a_y &= \frac{2}{3} & (\text{for semi-disks}), \\ a_x &= \frac{3}{2} + \frac{4}{\pi^2}, & a_y &= \frac{1}{2} & (\text{for flashing cuts}). \end{aligned} \quad (14)$$

The quantity  $\bar{\tau}_c$  is determined by gas statistics:

$$\frac{1}{\bar{\tau}_c} = \frac{\int_0^\infty d\varepsilon (f^{(0)'})^2 (\varepsilon/\tau_c(\varepsilon))}{\int_0^\infty d\varepsilon \varepsilon (f^{(0)'})^2},$$

where prime notes the derivative over the energy  $\varepsilon$ .

In the case of static cuts or semi-disks  $1/\tau_c(\varepsilon) \propto \varepsilon^s$  with  $s = 1/2$ . So one can write  $\bar{\tau}_c = \tau_c(\varepsilon_F)$  (strongly degenerate Fermi case) and  $\bar{\tau}_c = 4\sqrt{2/\pi} \tau_c(T)/3$  (Boltzmann case);  $s = 1/2$  for fixed obstacles and  $s = 0$  for flashing cuts (in this case  $\tau_c(\varepsilon) = \text{const}$ ).

The physical origin of Eqs. (12) and (13) is a very quick relaxation of higher angular momenta harmonics as compared to the first harmonic relaxation. As a result the conductivity has different values at low temperature, when  $\tau_{ee} \gg \tau_{el}$  and at high temperature when  $\tau_{ee} \ll \tau_{el}$ . In both limits the conductivity does not depend on e-e interaction, but has different values. In the case of the Fermi distribution the conductivity changes from low temperature value where  $\tau_{ee} \gg \tau_{el}$  to high temperature value where  $\tau_{ee} \ll \tau_{el}$ . We should emphasize that the transition between these two values is ruled by the ratio  $\tau_{ee}/\tau_{el}$  rather than by the ratio of temperature  $T$  to the Fermi energy  $E_F$ . The transition temperature  $T_0$  can be estimated by equating  $e$ - $e$  relaxation time to the relaxation time given by elastic scattering. In clean samples with high mobility the transition corresponds to a rather low temperature  $T_0 \sim E_F/\alpha \sqrt{\lambda_F/l_p}$ , where  $\alpha = (e^*)^2/\hbar v_F$  is the dimensionless e-e interaction constant,  $\lambda_F$  and  $v_F$  are the Fermi wavelength and velocity  $l_p$  is the elastic mean free path. For  $E_F = 0.01 \text{ eV}$ ,  $\lambda_F \approx 10 \text{ nm}$ ,  $\alpha = 0.5$ ,  $l_p \sim 10^{-4} \text{ cm}$ ,  $T_0 \sim 10 \text{ K}$ .

From Eq.(12) one can write the expression for ratio of static conductivities  $\sigma_{yy}/\sigma_{xx}$ :

$$\sigma_{yy}/\sigma_{xx} = \tau_y/\tau_x = a_x/a_y. \quad (15)$$

In case of flashing cuts this ratio is equal to  $3 + 8/\pi^2 \approx 3.81$  (see Eq. (14)). For such scatterers the problem of linear conductivity is solved exactly also in the limit of absence of e-e interaction (see e.g. [18]). Using Eq.(8), we find  $\sigma_{ii} = n_e e^2 \tau_{ci}/m$ ,  $b_x = 1/2$ ,  $b_y = 3/2$ . Thus, in this case  $\sigma_{yy}/\sigma_{xx} = 3$ . Hence, for example, for this flashing cuts model the ratio  $\sigma_{yy}/\sigma_{xx} = 3$  is changed significantly when the temperature is changed from  $T < T_0$  to  $T > T_0$ .

### Quadratic response

The stationary ratchet flow appears in the second order of  $ac$ -force  $F$ . In this case we can operate in a similar

way as before. The nonlinearity occurs due to the field term in the kinetic equation and nonlinear e-e collision operator:

$$\begin{aligned} & \partial_t f^{(2)} - (\hat{I}_{el} + \hat{I}'_{ee})(f^{(2)}) = \\ & -(\mathbf{F}(t)\partial_{\mathbf{p}})f^{(1)} + \hat{I}''_{ee}(f^{(1)} * f^{(1)}). \end{aligned} \quad (16)$$

The projection of anisotropic elastic collision operator onto the vector functions kills the third rank tensor needed for photogalvanic current. So inclusion of anisotropy should be done a bit more accurately. In short the stationary ratchet current is generated in a following way. The oscillating distribution function with vector anisotropy is converted by nonlinear *e-e* interactions to the static second angular harmonics which in turn is partially suppressed by linear *e-e* interactions and then is transformed to the static vector anisotropy by anisotropic elastic collisions. The main contribution to the stationary flow reads

$$j_i = \frac{1}{S} \text{Re} \sum_{\mathbf{p}} v_i \hat{I}^{-1} \hat{I}^{(-)} \hat{I}^{-1} \hat{I}_{ee}^{(2)} (f_{-\omega}^{(1)} * f_{\omega}^{(1)}), \quad (17)$$

The Eq.(17) has simplified form in accordance with the smallness of the elastic antisymmetric operator  $\hat{I}^{(-)}$  as compared with the inelastic scattering ( $\hat{I}^{(-)}$  obligatory contains higher angular harmonics). The subsequent simplifications include: the substitution of  $\hat{I}'_{ee}$  instead of  $\hat{I}''_{ee}$ , according Eq. (4); use of the fact that inverse operators  $\hat{I}^{-1}$  do not contain antisymmetric operators; the cancellation of  $\hat{I}^{-1} \hat{I}_{ee}^{(1)}$  acting on the second angular harmonics; the replacement of the left operator  $\hat{I}^{-1}$  (taking into account summation with  $v_i$ ) by the inverse projected operator. As a result, we arrive at

$$v_{f,i} = -\frac{1}{2} C \sum_{j,k} a_{jki} \tau_i \text{Re}(\tau_{\omega j} \tau_{\omega k}^* F_{\omega j} F_{\omega k}^*). \quad (18)$$

Here  $\varepsilon = mv^2/2$  is the particle energy,  $a_{ijk} = \langle v_i v_j \hat{I}^{(-)} v_k \rangle > \tau_c/v^3$  is a numerical tensor, characterizing the asymmetry of scatterers ( $\langle \dots \rangle$  stands for average over angles in the momentum space), prime again means the derivative over particle energy,  $1/\tau_{\omega i} = -i\omega + 1/\tau_i$ . For the specific cases of our models we obtain

$$\begin{aligned} a_{xxx} &= \frac{1}{48}, \quad a_{xyy} = -\frac{1}{16} \quad (\text{for static cuts}), \\ a_{xxx} &= -a_{xyy} = \frac{1}{12}, \quad (\text{for semi-disks}), \\ a_{xxx} &= \frac{1}{6\pi}, \quad a_{xyy} = -\frac{1}{3\pi}, \quad (\text{for flashing cuts}). \end{aligned} \quad (19)$$

For  $C$  we have:

$$C = \frac{\int_0^\infty d\varepsilon (f^{(0)'})^2 (v^3/\tau_c)'}{\int_0^\infty d\varepsilon \varepsilon (f^{(0)'})^2}.$$

In the case of static cuts or semi-disks  $C = (3/2 + s)v_F^3/(\tau_c(\varepsilon_F)\varepsilon_F^2)$  (strongly degenerate Fermi case) and

$C = 2d_s(3/2 + s)/(2^{1/2+s}m\tau_c(T)\sqrt{mT})$  (Boltzmann case);  $s = 1/2, d_s = 1$  for fixed obstacles and  $s = 0, d_0 = \sqrt{\pi}/2$  for flashing cuts (in this case  $\tau_c(\varepsilon) = \text{const}$ ).

To compare with results of numerical calculations it is convenient to write expressions for ratchet velocity components. For the linear polarization of monochromatic force we obtain

$$\begin{aligned} v_{fx}/v_T &= -B(Fv_T\bar{\tau}_c/T)^2 a_{xxx} \times \\ & [\cos^2 \theta / (a_x^3(1 + \omega^2\tau_x^2)) - \sin^2 \theta / (a_x a_y^2(1 + \omega^2\tau_y^2))] \\ v_{fy}/v_T &= -B(Fv_T\bar{\tau}_c/T)^2 a_{xyy} \times \\ & \sin(2\theta)(1 + \omega^2\tau_x\tau_y)/(a_x a_y^2(1 + \omega^2\tau_x^2)(1 + \omega^2\tau_y^2)), \end{aligned} \quad (20)$$

where  $B = CT^2\bar{\tau}_c/2v_T^3$  and we remind that  $\tau_i = \bar{\tau}_c/a_i$ . For the flashing cuts model we have  $\tau_c = \bar{\tau}_c$ ,  $a_{xxx} = 1/6\pi$ ,  $a_{xyy} = -1/3\pi$ ,  $a_x = 3/2 + 4/\pi^2$ ,  $a_y = 1/2$ ,  $C = 2\sqrt{\pi}/(2m\tau_c\sqrt{mT})$ ,  $\tau_c = \text{const}$  and for the semi-disks model  $a_{xxx} = -a_{xyy} = 1/12$ ,  $a_x = 2/3 + 8/3\pi$ ,  $a_y = 2/3$ ,  $C = 2/(m\bar{\tau}_c\sqrt{mT})$ ,  $\bar{\tau}_c \propto T^{-1/2}$ . Here we give the results for the Boltzmann distribution  $f^{(0)}$ , but similar calculations work for other  $f^{(0)}$ , e.g. for the Fermi-Dirac distribution. We also give a simplified derivation of the ratchet flow in the Appendix. It is based on the local equilibrium distribution and give the same results as Eqs. (20).

The opposite limit in absence *e-e* interactions was analytically studied for the cases of static cuts [16] (exactly) and approximately, for weak anisotropy, for static cuts or semi-disks [18]. It is important to emphasize that in both limits of weak and strong *e-e* interactions the current does not contain the strength of interactions. The transition between the regimes occurs when the interparticle scattering rate becomes comparable with the rate elastic scattering on anti-dots and impurities.

## IV NUMERICAL RESULTS

For the flashing cuts model the theory (20) gives a good description of numerical data (see Fig. 4). For the semi-disks model the agreement between the theory and numerical simulations (Fig. 3, top) is less accurate, e.g. 4th  $\theta$ -harmonic for  $v_{f,x}$  is absent in (20). To understand the origins of this difference we present the map of local flow velocities at various polarizations  $\theta$  in Fig. 5. For  $\theta = 0$  the results clearly show the appearance of turbulent flow with two vertexes behind the semi-disk. When the interaction scattering time  $\tau_K$  is increased by a factor 25 the interaction and turbulence practically disappear and the average local flow becomes laminar (see Fig. 5 top left and bottom right panels). At the same time even with strong interactions the flow has much more laminar structure for  $\theta = \pi/4$  (Fig. 5, top right panel) when the absolute value of the total ratchet velocity has its maximal value (see Fig. 3 top panel). Thus the ratchet flow

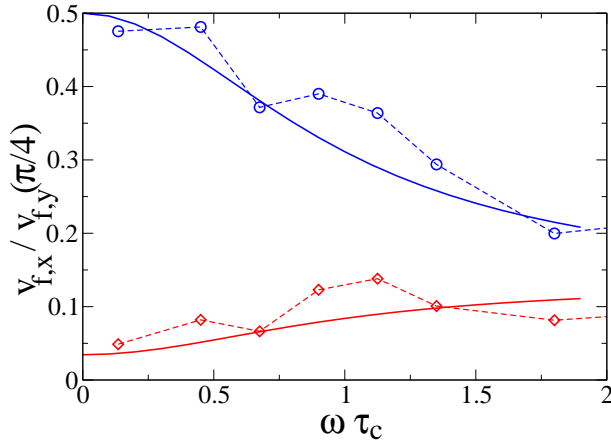


FIG. 4: (Color online) Comparison between theory (20) (full curves, no adjustable parameters) and numerical data for interacting particles in the flashing cuts model (symbols); circles are for  $v_{f,x}$  and  $\theta = \pi/2$  (here  $v_{f,x} > 0$ ), diamonds are for  $|v_{f,x}|$  and  $\theta = 0$  (here  $v_{f,x} < 0$  and we use the absolute value of  $v_{f,x}$  in the ratio  $v_{f,x}/v_{f,y}(\pi/4)$ );  $v_{f,y}$  is taken at  $\theta = \pi/4$ ; other parameters are as in Fig. 2, top panel.

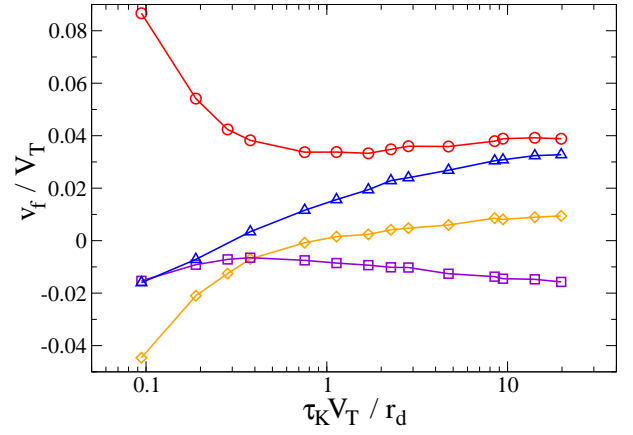


FIG. 6: (color online) Dependence of the ratchet velocity  $v_f$  on the Kapral interaction scattering time  $\tau_K$  in the semi-disk model, numerical data are shown by symbols:  $v_{f,y}/v_T$  (red circles) and  $v_{f,x}/v_T$  (yellow diamonds) for  $\theta = \pi/4$ ;  $v_{f,x}/v_T$  (violet squares) for  $\theta = 0$ ;  $v_{f,x}/v_T$  (blue triangles) for  $\theta = \pi/2$ ; other parameters are as in Fig. 3, top panel, curves are drawn to adapt an eye.

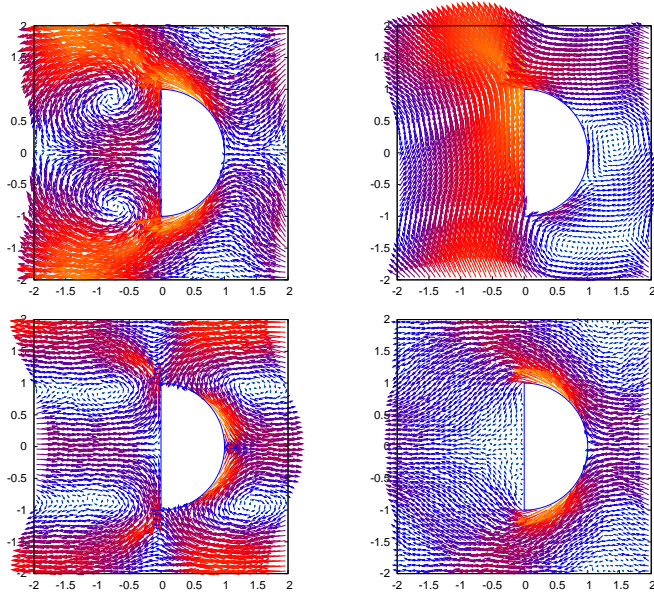


FIG. 5: (Color online) Map of local averaged velocities in  $(x/R, y/R)$  plane of the semi-disks model for parameters of Fig. 3 (top panel) at  $\theta = 0$  (top left);  $\theta = \pi/4$  (top right);  $\theta = \pi/2$  (bottom left);  $\theta = 0$  and 25 times increased interaction time compared to other panels ( $\tau_K/\tau_H = 0.5$ ,  $\tau_K v_T/r_d = 4.7$  point in Fig. 6). The velocities are shown by arrows which size is proportional to the velocity amplitude, which is also indicated by color (from yellow/gray for large to blue/black for small amplitudes).

of interacting particles has certain similarities with a hydrodynamic flow of the Navier-Stokes equation around semi-disk body [26]. However, for  $\theta = \pi/2$  the ratchet flow is composed from two alternative flows moving in opposite directions at the cell boundaries and the semi-disk center (Fig. 5, bottom left panel), such a rather flow

is different from hydrodynamic flows with fixed velocity far from the body. For a qualitative description of the turbulent flow we may argue that the turbulence leads to a difference of pressures on different sides of the scatterer producing different resistances for different flow directions. This generates the ratchet flow for the *ac*-force driving. In general the kinetic description is applicable when the interaction scattering length is large compared to the scatterer size, e.g.  $v_T \tau_K > r_d$  for semi-disks. At small values of  $\tau_K$  this condition is broken (Figs. 3,5) and we have transition to the hydrodynamic like regime where the theory (20) gives only approximate description. For the flashing cuts model the kinetic description remains always valid since the size of scatterer is zero.

The dependence of the ratchet velocity on the interaction scattering time  $\tau_K$  is shown in Fig. 6. The increase of interactions (small  $\tau_K$ ) can change the sign of the flow in  $x$ -direction that is in a qualitative agreement with the theory (20). For weak interactions the flows are opposite in  $x$  for polarization  $\theta = 0$  and  $\theta = \pi/2$  while at strong interactions they are collinear. Thus in 2DEG in AlGaAs/GaAs heterojunctions where interactions are relatively weak ( $r_s \sim 1$ ) the flows are opposite for two polarizations in agreement with the experiment [19], but for other materials with stronger interactions (e.g. SiGe with  $r_s \approx 6$ ) the flows may become collinear. We also note that at strong interactions the rescaled ratchet characteristics are not sensible to the temperature variation that indicates that we have an effective liquid flow with temperature independent viscosity.



## V DISCUSSION

In conclusion, our extensive numerical simulations show that even in the regime of strong interactions between particles a stationary ratchet flow is generated by monochromatic driving in the asymmetric periodic arrays. The obtained result are well described by the analytical theory based on the kinetic equation for strongly interacting particles. It is interesting to note that for asymmetric arrays the tensor of conductivity becomes temperature dependent due to interplay of interactions and relaxation of high momentum harmonics (see Eq. (15) and discussion there). It would be interesting to investigate the effects of interactions on ratchet transport in experiments similar to those of [19].

This research is supported in part by the ANR projects MICONANO and NANOTERRA (France) and RFBR NN 08-02-00152-a, 08-02-00506-a (Russian Federation).

## APPENDIX

Here, on the example of the flashing cuts model we give a more simple and heuristic derivation of the ratchet flow compared to the exact kinetic equation approach (1). In the regime of very strong interactions we can assume that the ensemble of particles is in a local equilibrium state and hence the distribution function can be written as

$$f(\mathbf{v}, t) = f_0(\mathbf{v} - \mathbf{v}_0(t)) \quad (\text{A-1})$$

where  $\mathbf{v}_0(t)$  is the instantaneous velocity of the center of mass. We put here the particle mass  $m = 1$ . It is assumed that the interactions give rapid relaxation to the local equilibrium distribution  $f_0(\mathbf{v} - \mathbf{v}_0(t))$ . The matrix of conductivity can be determined from the momentum balance between acceleration created by a small applied static force  $\mathbf{F}$  and momentum loss on the asymmetric cut scatterer:

$$\frac{d\mathbf{p}}{dt} = \mathbf{F} - \frac{1}{\tau_c} \langle \mathbf{V}_c(\mathbf{v}) f_0(\mathbf{v} - \mathbf{v}_0) \rangle - \mathbf{v}_0 = 0, \quad (\text{A-2})$$

where  $\mathbf{V}_c(\mathbf{v})$  is the vector of average velocity after a scattering with the incident velocity  $\mathbf{v}$ . It is expressed via the scattering probability  $W(\mathbf{v}', \mathbf{v})$  (see the main text above) as  $\mathbf{V}_c(\mathbf{v}) = \int d\mathbf{v}' W(\mathbf{v}', \mathbf{v}) \mathbf{v}'$ . This gives the relation

$$\langle \mathbf{V}_c(\mathbf{v}) f_0(\mathbf{v} - \mathbf{v}_0) \rangle = \int d\mathbf{v} \left( \frac{2|\mathbf{v}|\theta(-v_x)}{\pi} - v_x \theta(v_x) \right) f_0(\mathbf{v} - \mathbf{v}_0) \quad (\text{A-3})$$

where  $\theta(v)$  is the Heaviside function. In the linear response regime we can expand in  $\mathbf{v}_0$  that gives  $f_0(\mathbf{v} - \mathbf{v}_0) = f_0(\mathbf{v}) + f_0(\mathbf{v}) \frac{\mathbf{v}\mathbf{v}_0}{T} + \dots$ . After integrating over the

Maxwell distribution  $f_0(\mathbf{v})$  we obtain

$$\begin{aligned} \langle \mathbf{V}_c(\mathbf{v}) f_0(\mathbf{v} - \mathbf{v}_0) \rangle &= \\ \int d\mathbf{v} \left( \frac{2|\mathbf{v}|\theta(-v_x)}{\pi} - v_x \theta(v_x) \right) f_0(\mathbf{v}) \frac{\mathbf{v}\mathbf{v}_0}{T} \\ &= \left( -\frac{8+\pi^2}{2\pi^2} v_{0,x}, \frac{1}{2} v_{0,y} \right) \end{aligned} \quad (\text{A-4})$$

where  $\mathbf{v}_0$  is the velocity of the stationary flow. Then the moment balance gives

$$\begin{pmatrix} v_{0,x} \\ v_{0,y} \end{pmatrix} = \tau_c \begin{pmatrix} \frac{2\pi^2}{8+3\pi^2} F_x \\ 2F_y \end{pmatrix} \quad (\text{A-5})$$

and therefore  $\sigma_{yy}/\sigma_{xx} = \tau_y/\tau_x = a_x/a_y = 3 + 8/\pi^2$  that is in agreement with the kinetic theory result given in the main text. It is interesting to note that for the noninteracting particles we have  $\sigma_{yy}/\sigma_{xx} = 3$  (see [18]).

To compute the ratchet flow we should expand the local velocity in Eq. (A-1) up to the second order in the driving force  $F$ :  $\mathbf{v}_0(t) = \hat{\tau}_i \mathbf{F}(t) + \mathbf{v}_f$ ,  $v_f = O(F^2)$  where  $\tau_i$  are the above values  $\tau_x, \tau_y$  given by the linear response; we note that second frequency harmonics  $e^{\pm i2\omega t}$  are eliminated by the time averaging. Then the time averaged distribution function is

$$\begin{aligned} f(\mathbf{v}) &= \langle f(\mathbf{v}, t) \rangle_t = \\ f_0(\mathbf{v}) &+ f_0(\mathbf{v}) \frac{\mathbf{v}\mathbf{v}_f}{T} + \frac{(\mathbf{v}\hat{\tau}_i \mathbf{F})^2 - T(\hat{\tau}_i \mathbf{F})^2}{4T^2} f_0(\mathbf{v}) \end{aligned} \quad (\text{A-6})$$

where  $f_0(\mathbf{v}) = \frac{1}{Z} \exp(-\frac{v^2}{2T})$  is the Maxwell distribution and  $\mathbf{v}_f$  is the average ratchet flow velocity. Again, the time averaged momentum balance equation reads

$$\langle \mathbf{V}_c(\mathbf{v}) f(\mathbf{v}) \rangle - \mathbf{v}_f = 0. \quad (\text{A-7})$$

Using Eq. (A-7) we obtain from the second term the contribution  $\langle \mathbf{V}_c(\mathbf{v}) f_0(\mathbf{v}) \frac{\mathbf{v}\mathbf{v}_f}{T} \rangle = ((1 - a_x)v_{fx}, (1 - a_y)v_{fy})$  which is similar to the linear response term. The integration of the third Gaussian term gives the additional contribution  $(F^2/8\sqrt{2\pi T})[(-\tau_x^2 \cos^2 \theta + \tau_y^2 \sin^2 \theta), 2\tau_x \tau_y \sin(2\theta)]$ . Finally we obtain

$$\begin{pmatrix} v_{fx} \\ v_{fy} \end{pmatrix} = \frac{F^2}{8\tau_c \sqrt{2\pi T}} \begin{pmatrix} -\tau_x^3 \cos^2 \theta + \tau_x \tau_y^2 \sin^2 \theta \\ 2\tau_x \tau_y^2 \sin(2\theta) \end{pmatrix} \quad (\text{A-8})$$

For  $\omega \rightarrow 0$  these expressions are in agreement with Eqs. (20) obtained by the kinetic equation theory.

- 
- [1] F. Jülicher, A. Ajdari, and J. Prost, Rev. Mod. Phys. **69**, 1269 (1997).
  - [2] P. Reimann, Phys. Rep. **361**, 57 (2002).
  - [3] P. Hänggi, and F. Marchesoni, arXiv:0807.1283[cond-mat] Rev. Mod. Phys. to appear (2008).

- [4] E. M. Baskin, L. I. Magarill, M. V. Entin, Sov. Phys.-Solid State **20**, 1403 (1978) [Fiz. Tver. Tela **20**, 2432 (1978)].
- [5] V. I. Belinicher, B. I. Sturman, Sov. Phys. Usp. **23**, 199 (1980) [Usp. Fiz. Nauk **130**, 415 (1980)].
- [6] V.L.Alperovich, V. I. Belinicher, V. N. Novikov, and A. S. Terekhov, JETP Lett. **31**, 546 (1980).
- [7] J.B. Majer, J. Peguiron, M. Grifoni, M. Tusveld, and J.E. Mooij, Phys. Rev. Lett. **90**, 056802 (2003); A. V. Ustinov, C. Coqui, A. Kemp, Y. Zolotaryuk, and M. Salerno, Phys. Rev. Lett. **93**, 087001 (2004).
- [8] S. Matthias and F. Müller, Nature **424**, 53 (2003).
- [9] V. Studer, A. Pepin, Y. Chen, and A. Ajdari, Analyst **129**, 944 (2004).
- [10] A. Lorke, S. Wimmer, B. Jager, J.P. Kotthaus, W. Wegscheider, and M. Bichler, Physica B **249-251**, 312 (1998).
- [11] H. Linke, T.E. Humphrey, A. Löfgren, A.O. Sushkov, R. Newbury, R.P. Taylor, and P. Omling, Science **286**, 2314 (1999).
- [12] A.M. Song, P. Omling, L. Samuelson, W. Seifert, I. Shorubalko, and H. Zirath, Appl. Phys. Lett. **79**, 1357 (2001).
- [13] P. Olbrich, E.L. Ivchenko, T. Feil, R. Ravash, S.D. Danilov, J. Allerdings, D. Weiss, S.D. Ganichev, preprint arXiv:0808.1983[cond-mat] (2008).
- [14] A.D.Chepelianskii, and D.L.Shepelyansky, Phys. Rev. B **71**, 052508 (2005).
- [15] G. Cristadoro, and D.L.Shepelyansky, Phys. Rev. E **71**, 036111 (2005).
- [16] M. V. Entin, L. I. Magarill, Phys. Rev. B **73**, 205206 (2006).
- [17] A.D.Chepelianskii, Eur. Phys. J. B **52**, 389 (2006).
- [18] A. D. Chepelianskii, M. V. Entin, L. I. Magarill and D. L. Shepelyansky, Eur. Phys. J. B **56**, 323 (2007).
- [19] S. Sassine, Y. Krupko, J.-C. Portal, Z. D. Kvon, R. Murali, K.P.Martin, G.Hill, and A.D.Wieck, Phys. Rev. B **78**, 045431 (2008).
- [20] E. Abrahams, S. V. Kravchenko, and M. P. Sarachik, Rev. Mod. Phys. **73**, 251 (2001).
- [21] D. van der Meer, P. Reimann, K. van der Weele, and D. Lohse, Phys. Rev. Lett. **92**, 184301 (2004).
- [22] D. E. Feldman, S. Scheidl, and V. M. Vinokur Phys. Rev. Lett. **94**, 186809 (2005); B. Braunecker, D. E. Feldman, and J. B. Marston, Phys. Rev. B **72**, 125311 (2005).
- [23] A. Malevanets, and R. Kapral, Lect. Notes Phys. (Springer) **640**, 116 (2004).
- [24] W. G. Hoover, *Time reversibility, computer simulation, and chaos*, World Scientific, Singapore (1999).
- [25] A. D. Chepelianskii, A. S. Pikovsky and D. L. Shepelyansky, Eur. Phys. J. B **60**, 225 (2007).
- [26] L. D. Landau and E. M. Lifshitz, *Hydrodynamics*, Nauka, Moskow (1986),